THE JOURNAL OF BIOLOGICAL CHEMISTRY VOL. 289, NO. 46, pp. 32153–32165, November 14, 2014
Published in the U.S.A.

DPP6 Domains Responsible for Its Localization and Function*

Received for publication, April 30, 2014, and in revised form, August 22, 2014 Published, JBC Papers in Press, September 4, 2014, DOI 10.1074/jbc.M114.578070

Lin Lin[1], **Laura K. Long, Michael M. Hatch, and Dax A. Hoffman**

From the Molecular Neurophysiology and Biophysics Section, Program in Developmental Neuroscience, Eunice Kennedy Shriver National Institute of Child Health and Human Development, National Institutes of Health, Bethesda, Maryland 20892

Background: DPP6, a transmembrane protein with a large extracellular domain, is an auxiliary subunit of Kv4.2 potassium channels.
Results: The extracellular domain is required for DPP6 export from the ER while intracellular domains impart the functional impact on Kv4.2.
Conclusion: Different DPP6 domains are responsible for its localization and function.
Significance: Understanding DPP6 function may provide insight into its role in neuronal development and disease.

Dipeptidyl peptidase-like protein 6 (DPP6) is an auxiliary subunit of the Kv4 family of voltage-gated K^+ channels known to enhance channel surface expression and potently accelerate their kinetics. DPP6 is a single transmembrane protein, which is structurally remarkable for its large extracellular domain. Included in this domain is a cysteine-rich motif, the function of which is unknown. Here we show that this cysteine-rich domain of DPP6 is required for its export from the ER and expression on the cell surface. Disulfide bridges formed at C349/C356 and C465/C468 of the cysteine-rich domain are necessary for the enhancement of Kv4.2 channel surface expression but not its interaction with Kv4.2 subunits. The short intracellular N-terminal and transmembrane domains of DPP6 associates with and accelerates the recovery from inactivation of Kv4.2, but the entire extracellular domain is necessary to enhance Kv4.2 surface expression and stabilization. Our findings show that the cysteine-rich domain of DPP6 plays an important role in protein folding of DPP6 that is required for transport of DPP6/Kv4.2 complexes out of the ER.

Dipeptidyl aminopeptidase-like protein 6, or DPP6[2] (also referred to as DPPX, BSPL, or potassium-channel accelerating factor KAF) (1), is a member of the prolyl oligopeptidase family of serine proteases. This family also includes proteins such as DPP8, DPP9, and most notably DPPIV (also known as CD26) (1, 2). Most of these proteases work to remove dipeptides from other regulatory proteins and peptides. CD26 in particular is important for the regulation of immune, metabolic, CNS, and inflammatory functions, mediated by its exopeptidase activity (3–5). However, DPP6 has a point mutation at the enzymatic serine (to aspartate), and is among those in the family that have lost their peptidase function. This group is often referred to as the dipeptidyl aminopeptidase-like proteins (DPPLs) (1, 6). The DPP6 gene encodes at least three different splice isoforms that diverge in the N-terminal domain. *In situ* hybridization of rat brain tissue showed that DPP6-S is the most prominent isoform in the CA1 region (7).

Structurally, DPP6 is a type II transmembrane protein that consists of a single transmembrane domain and a short intracellular N terminus. Strop *et al.* (2004) published the x-ray crystal structure of DPP6, illuminating many specific features of the protein. They found that two monomers of DPP6 associate to form a homodimer. Each monomer possesses an eight-bladed β-propeller and an α/β hydrolase domain, which both participate in dimer formation outside of the cell. By far the largest portion of the protein is the extracellular C terminus (803 aa).

The DPP6 protein structure is highly similar to the antigenic exopeptidase family member DPPIV/CD26 (32% sequence identity and 50% sequence similarity) (8). They share large extracellular C termini that are divisible into three domains. In DPP6, the first extracellular domain (231aa) is a glycosylation domain containing seven n-glycosylation sites. These sites occur primarily in the β propeller, with only one site in the α/β hydrolase domain. The second extracellular domain (193 aa) is a cysteine-rich domain along the middle blades of the C terminus. Each monomer contains four disulfide bridges in this domain. CD26 also contains these disulfide bonds, along with a fifth bridge in blade 6 of its β-propeller. The third, "aminopeptidase" domain (134 aa) is at the end of the C terminus and contains the DPP6 serine mutation. Strop *et al.* (2004) speculate that this change may have actually resulted in the gain of function as a potassium channel accelerating factor. They also note that DPP6 contains several β-propeller motifs that "commonly act as scaffolds for protein-protein interactions," and may have additional unidentified binding partners. DPP6 similarity to CD26 goes beyond structure. CD26, like DPP6, also binds the extracellular matrix. *In vitro* binding assays have shown that CD26 binds to collagens I and II at its cysteine-rich domain, and also binds to fibronectin (9–11).

DPP6 is mostly studied as an auxiliary subunit of voltage-gated K^+ channels of the Kv4 family. Kv4 channels, along with channels from the Kv1 family, primarily underlie the transient subthreshold-activating A-type current (I_A) in neurons. I_A plays a major role in neuronal excitability by opposing depolar-

* This work was supported by the Intramural Research Program of the Eunice Kennedy Shriver National Institute of Child Health and Human Development, National Institutes of Health.
[1] To whom correspondence should be addressed: 35 Lincoln Dr., MSC 3715, Bldg 35, Room 3C-908, Bethesda, MD 20892-3715. E-mail: linl2@mail.nih.gov.
[2] The abbreviations used are: DPP, dipeptidyl aminopeptidase-like protein; KChIP, Kv channel-interacting protein; IR-DIC, infrared differential interference contrast; ER, endoplasmic reticulum.

ization, dampening action potential (AP) initiation and frequency (12). Kv4.2 is the main α subunit for channels of this type in the somatodendritic regions of CA1 hippocampal neurons (13). As Kv4.2 is highly expressed in distal CA1 dendrites, these channels control backpropagation of APs into dendrites, significantly impacting synaptic plasticity (13–15).

A-type K^+ channels underlying the dendritic A-current in CA1 neurons appear to exist as a complex consisting of three main proteins: the pore-forming Kv4 subunit along with two auxiliary proteins, a Kv channel-interacting protein (KChIP) and a dipeptidyl aminopeptidase-like protein (DPPL) (16, 17). The expression of all three subunits is required to reproduce native-like I_A currents in heterologous systems. In CA1 pyramidal hippocampal neurons, these channels are primarily Kv4.2, KChIP2, KChIP4, and DPP6 (18, 19).

In heterologous co-expression and knockdown studies in neurons, DPP6 increases Kv4.2 surface expression and accelerates channel activation, inactivation, and recovery from inactivation (20, 21). In addition, we have recently found that DPP6 is important for localizing Kv4.2 to the distal dendrites in CA1 neurons, impacting dendritic excitability synaptic and plasticity (22). DPP6 knock-out mice exhibited hyperexcitable dendrites with enhanced dendritic AP back-propagation, calcium electrogenesis, and induction of synaptic long-term potentiation.

DPP6 effects on Kv4.2 make it an important protein to study to better understand such crucial neuronal processes as synaptic integration and plasticity. However, recent reports suggest that DPP6 may have additional roles independent of that as a Kv4 auxiliary subunit (11, 23, 24). Recently, we reported a novel, Kv4-independent role for DPP6 in neuronal development. Electrophysiological, molecular, and imaging experiments showed that DPP6 binds to the extracellular matrix and has a significant impact on filopodia formation and stability, consequently affecting dendritic arborization, spine density, and synaptic function in CA1 neurons (11). Further characterization of DPP6's structure and function may contribute to our understanding of these processes and uncover possible roles in neuropsychiatric pathologies where the DPP6 gene has been implicated, including autism spectrum disorders (25, 26), mental retardation (27), and amyotrophic lateral sclerosis (28, 29).

Little is known about the intracellular trafficking of DPP6. However, a recent study showed that DPP6 expression and stability are not dependent on Kv4.2 (23). DPP6 expression levels are completely unaffected by the absence of Kv4.2 in mouse cortex, and DPP6 protein levels appear to be stable without Kv4.2. These results indicate that DPP6 has the capacity to traffic independently of Kv4.2, but this trafficking has not been examined in the literature. We show here, using live imaging and biochemistry that the cysteine-rich domain is important for DPP6 exit from the ER and localization to the cell surface. We also show that while the extracellular domain of DPP6 is important for enhancing the surface expression of Kv4.2, the short intracellular N-terminal plus transmembrane domains of DPP6 are necessary for it to associate with and accelerate the properties of Kv4.2.

EXPERIMENTAL PROCEDURES

Constructs DPP6 and Deletions—DPP6-GFP wildtype construct was prepared by PCR using the primers 5′-GGTGGTCTCGAGATGACCACGCCCAAGGAGC (forward) and 5′-GGTGGTCTGCAGGTCCTCCTCCTCGTCCTCTTTC (reverse) on construct pcDNA3-DPP6 (kindly provided by Dr. Rudy, NYU School Medicine, New York) and subcloned into the XhoI-PstI sites of the pEGFP-N1 vector, and confirmed by sequencing analysis. Cysteine point mutation of DPP6-C349A/C356A including C349A and C356A were made by overlapping PCR. DPP6-D-Pep, DPP6-D-Pep+Cys, DPP6-D-Extra deletion constructs were made by PCR using the same forward primer 5′-CGCTCGAGATGACCACCGCCAAGGAGCCCAGC and different reverse primers 5′-CGCTGCAGCCTCTCTGACACGCTCTGACTCCC; 5′-CGCTGCAGGTGGTAGGGCTTCACAGTGGG and 5′-CGCTGCAGCAGCAGGATGACTGAGGTGAC on the construct DPP6-GFP and subcloned into pEGFP-N1 vector. The construct of DPP6-D32 deletion was made by using the primers 5′-CGCTCGAGATGGGAATCGCCATTGCACTGCTTGTC (forward) and 5′-CGCTGCAGGTCCTCCTCCTCGTCCTCTTTCGC (reverse). DPP6-D54 construct was made by using the primer 5′-CGCTCGAGATGGGCCTGACCCCAGCGGAAGATACCAGTC (forward) and same reverse primer as deletion DPP6-D32. All the constructs were confirmed by sequencing analysis. KChIP2a construct was kindly provided by Dr. Pfaffinger at Baylor College of Medicine, Houston, Texas.

Live Imaging and Measurements—HEK cells, which have an elevated morphology, were used in all live imaging experiments. HEK cells transfected with DPP6-WT or mutations and either ER-DsRed or membrane mCherry markers, after 24 h, live image with a Zeiss LSM 510 confocal microscope. Each coverslip was kept at 37 ° C until use, and was only used for imaging over a period of 15 min after being placed in the microscope with Invitrogen Leibovitz's (1×) L-15 Medium. Measure the intensity plot along the line drawn.

Co-immunoprecipitation and Western Blotting—To examine the DPP6 binding sites with Kv4.2, we performed co-immunoprecipitation (Co-IP) experiments in COS7 cells co-transfected with various DPP6 and Kv4.2 constructs for 24–48 h. Cells were lysed in lysis buffer: 150 mM NaCl, 20 mM Tris-HCl, 1% Nonidet P-40, and protease inhibitor mixture (Roche, Indianapolis, IN). Anti-DPP6 (2 μg/500 μg protein, Abcam, Cambridge, MA), IgG (Invitrogen) as nonspecific control was then added to the lysate. The mixture was then incubated and rotated at 4 °C overnight. The antibody-antigen complex was immobilized by adsorption onto 50 μl of immobilized protein A (Pierce) and incubated for 2 h at room temperature. The protein-bead mixtures were washed 6× with lysis buffer. The beads were resuspended in reducing SDS sample buffer and analyzed on 10% Bis-Tris SDS-polyacrylamide gels. The separated proteins were immunoblotted using DPP6 (1:2000) or Kv4.2 antibody (1:2000, NeuroMab, Davis, CA) and visualized by Alexa Fluor 680 secondary antibody (1:10,000, Invitrogen) and Alexa Fluor 800 secondary antibody (1:10,000, Rockland, Gilbertsville, PA). Immunoreactivity was detected with the Odyssey infrared imaging system (LI-COR Biosciences, Lin-

coln, Nebraska). Quantification of results was performed using Odyssey software (LI-COR Biosciences, Lincoln, Nebraska).

Biotinylation Assays—Biotinylation assays were performed as previously described (15). Briefly, transfected COS7 cells were rinsed with ice-cold PBS, surface protein were biotinylated with 1.5 mg/ml sulfo-NHS-SS-biotin reagent (Pierce) in PBS for 30 min on ice. Unbound biotin was quenched with cold 50 mM glycine in PBS. Cells were lysed with ice-cold lysis buffer: 150 mM NaCl, 20 mM Tris-HCl, 1% Nonidet P-40, and protease inhibitor mixture (Roche, Indianapolis, IN), sonicated, and centrifuged at 12,000 × *g* for 10 min. Cell lysates were incubated overnight at 4 °C with immobilized-Streptavidin-agarose beads (Pierce); unbound protein was removed from the beads with 5 washes in lysis buffer. The bound proteins were eluted with 2× SDS sample buffer. Surface-expressed proteins were separated by electrophoresis on 10% Tris-bis SDS-PAGE (Invitrogen, Carlsbad, CA) and transferred to PVDF membranes. Western blots were probed with the following antibodies: mouse anti-Kv4.2 (1:2000, NeuroMab, Davis, CA), rabbit anti-DPP6 (1:2000, Abcam, Cambridge, MA), mouse anti-GAPDH (1:1000, Calbiochem, San Diego, CA). Secondary antibodies conjugated to infrared dyes (Rockland Immunochemicals, Gilbertsville, PA) were detected using Odyssey infrared imaging system (LI-COR Biosciences, Lincoln, NE). Quantification of results was performed using Odyssey software.

Electrophysiology—HEK 293 cells were co-transfected with Kv4.2 (0.5 μg) and DPP6 or one of its mutations (0.5 μg) in 35-mm dishes using the Xtreme Gene 9 system (Roche Applied Science, Indianapolis, IN). For control recordings, Kv4.2 (0.5 μg) was co-transfected with empty vector (0.5 μg). Transfected cells were re-plated onto glass coverslips and recordings were made 16 to 20 h after transfection. Coverslips containing transfected HEK 293 cells were submerged in the recording chamber and exposed to a continuous flow of ACSF consisting of the following (mM): 145 NaCl, 3 KCl, 2 $CaCl_2$, 2 $MgCl_2$, 8 glucose, 10 HEPES. An infrared differential interference contrast (IR-DIC) videomicroscopy system (Zeiss Instruments, Diagnostic Instruments) was used to visualize cells. Patch pipettes were pulled from thick-walled borosilicate glass (Warner Instruments) to achieve a tip resistance of 2–5 MΩ. Pipettes were filled with an internal solution containing (mM): 146.5 K-gluconate, 7.5 KCl, 9 NaCl, 10 HEPES, 0.2 EGTA, and 1 $MgCl_2$. Whole-cell voltage clamp recordings were made using a Multiclamp 700B amplifier (Molecular Devices) and Clampex 10.1 software (Molecular Devices). Signals were digitized at 10 kHz with Digidata 1440A (Molecular Devices) and filtered at 2 kHz. All recordings were performed at room temperature, and recordings with cell capacitances less than 7 pF were excluded.

During the current density experiments, cells were initially held at −60 mv followed by a 400 ms pulse at −120 mv and then a 500 ms pulse at +60 mv to elicit the A-type current. This protocol was repeated 9 times for each cell. This protocol was also used to measure the A-type current of HEK 293T cells co-transfected with Kv4.2, KChIP2a, and in some cases either DPP6 or one of its mutations. The nine sweeps were averaged to form a trace from which the peak amplitude of I_A was calculated. This amplitude was then divided by the cell capacitance to obtain the current density (pA/pF).

For the recovery experiments, HEK 293 cells were co-transfected with Kv4.2 (0.5 μg) and DPP6-WT or DPP6-D-extra (0.5 μg). Cells were prepared for recording in the same manner as above. Cells were initially held at −60 mv followed by a 400 ms pulse to −100 mv and then a 400 ms pulse to +60 mv. After this induction of I_A,a second induction protocol was given 5,10, 15, 20, 25, 100, 200, or 500 ms later. At the end of each sweep the cell was given a 400 ms pulse to −100 mv, and then returned to −60 mv for 200 ms. This was repeated three times for each cell. Percent recovery was calculated by dividing the peak amplitude of each secondary current the initial peak I_A.

All recordings were analyzed using Clampfit 10.1 (Molecular Devices), Microsoft Excel, and Igor Pro 6.02A (WaveMetrics). All values are expressed as means ± S.E. Statistical significance was evaluated using Student's *t* test (unpaired, two tails) or ANOVA with Dunnett's *post hoc* multiple comparison test when comparing values against a basal control.

RESULTS

The Cysteine-rich Domain of DPP6 Is Required for ER-to-Membrane Transport—To investigate the functional roles of each extracellular DPP6 domain, we generated three truncation mutants: 1) "DPP6-D-Pep" with the aminopeptidase domain is deleted, 2) "DPP6-D-Pep+Cys" with both the cysteine-rich and aminopeptidase domains are deleted, and 3) "DPP6-D-Extra" with the entire extracellular domain is deleted, including the glycosylation, cysteine-rich, and aminopeptidase domains (Fig. 1*A*).

We began by examining the effect of the extracellular domain deletions on membrane localization. HEK293 cells were co-transfected with DPP6-WT or deletion mutants and a membrane marker (Mem-mCherry), which encodes a fusion protein consisting of the N-terminal 20 amino acids of neuromodulin tagged with mCherry red fluorescent protein. Live-cell images were captured 24 h after transfection. We found DPP6-WT to be expressed in the plasma membrane, showing colocalization with the membrane marker (Fig. 1*B*). DPP6-D-Pep showed similar expression as DPP6-WT (Fig. 1*D*). However, deletion of the cysteine-rich domain (DPP6-D-Pep+Cys) showed an intracellular expression pattern (Fig. 1*F*). Interestingly, DPP6-D-Extra, which is missing the entire extracellular domain, appears to have retained membrane expression, as demonstrated by colocalization with the membrane marker (Fig. 1*H*).

We quantified these mutation effects on DPP6 surface membrane expression with a biotinylation assay. COS7 cells were transfected with DPP6-WT or the C-terminal deletions (Fig. 1, *J* and *K*). DPP6-WT and deletions DPP6-D-Pep and DPP6-D-Extra showed similar levels of membrane expression as suggested in the live imaging experiments. Mutation DPP6-D-Pep+Cys, however, showed only 40% of WT surface expression (Fig. 1*K*, $p < 0.05$). Together, these results suggest that the cysteine-rich domain of DPP6 may be important for proper folding of the DPP6 extracellular domain, which is critical to its forward trafficking to the plasma membrane.

In the next experiment we examined the intracellular expression of the extracellular DPP6 mutations by co-expressing them in HEK293 cells with an ER marker labeled with Ds-Red to see if the poor surface expression of DPP6-D-Pep+Cys was due to

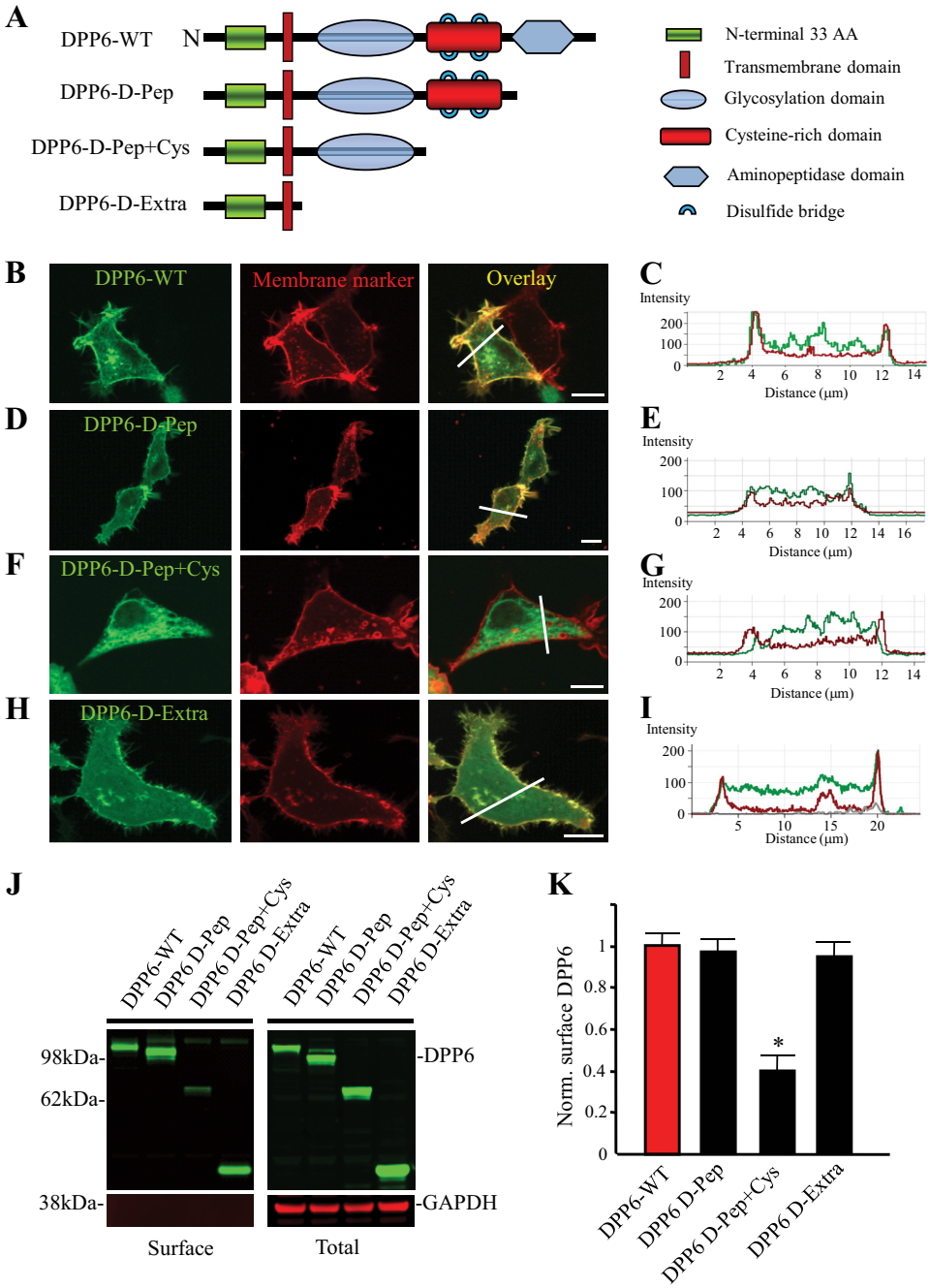

FIGURE 1. **The cysteine-rich domain of DPP6 is important for its membrane surface expression.** *A*, domain structures of wild type DPP6 and the C-terminal truncation deletions used in this study. *B–I*, live cell imaging of HEK293 cells co-transfected with DPP6-GFP-WT or mutant construct (*green*) and a membrane marker labeled with mCherry (*red*). Scale bars represent 10 μm. *B*, DPP6-WT expressed primarily in the membrane, co-localized with the membrane marker. *D*, DPP6-D-Pep expressed in the membrane similar to DPP6-WT in *B*. *F*, DPP6-D-Pep+Cys remains in the ER and does not co-localize with membrane maker. *H*, surprisingly, DPP6-D-Extra is distributed more at the membrane and co-localized with membrane marker and less in intracellular ER/Golgi compartment. An intensity plot along the white line is shown in *C*, *E*, *G*, and *I*. *J*, surface expression of DPP6-WT and deletions was measured with a biotinylation assay in overexpressed COS7 cells. Results showed that DPP6-WT, D-Pep, and D-Extra express robustly on the surface, but by comparison D-Pep+Cys has much less surface expression. GAPDH served as a loading control and the surface negative control. *K*, pooled surface biotinylation data ($n = 5$), normalized to total protein level of DPP6. Membrane expression of DPP6-D-Pep+Cys is significantly lower than other conditions. Error bars represent S.E.

ER retention (Fig. 2). Accordingly, we did find that this mutation colocalized with the ER marker (Fig. 2*E*), while DPP6-WT and the other mutations showed less ER expression (Fig. 2, *A*, *C*, and *G*).

C349/C356 and C465/C468 Disulfide Bridges Are Key to DPP6 Forward Trafficking—Given our results showing that the cysteine-rich domain is necessary for DPP6 transport out of the ER, and since disulfide bonds play an important role in the folding and stability of proteins, we hypothesized that the two disulfide bridges formed at C349/C356 and C465/C468 have key roles in the proper folding of DPP6. We made cysteine point mutations at DPP6-C349A/C356A and C465A/C468A (Fig. 3*A*), and performed biotinylation and live imaging assays. The live imaging data (Fig. 3*B*) and intensity plots (Fig. 3*C*) shown

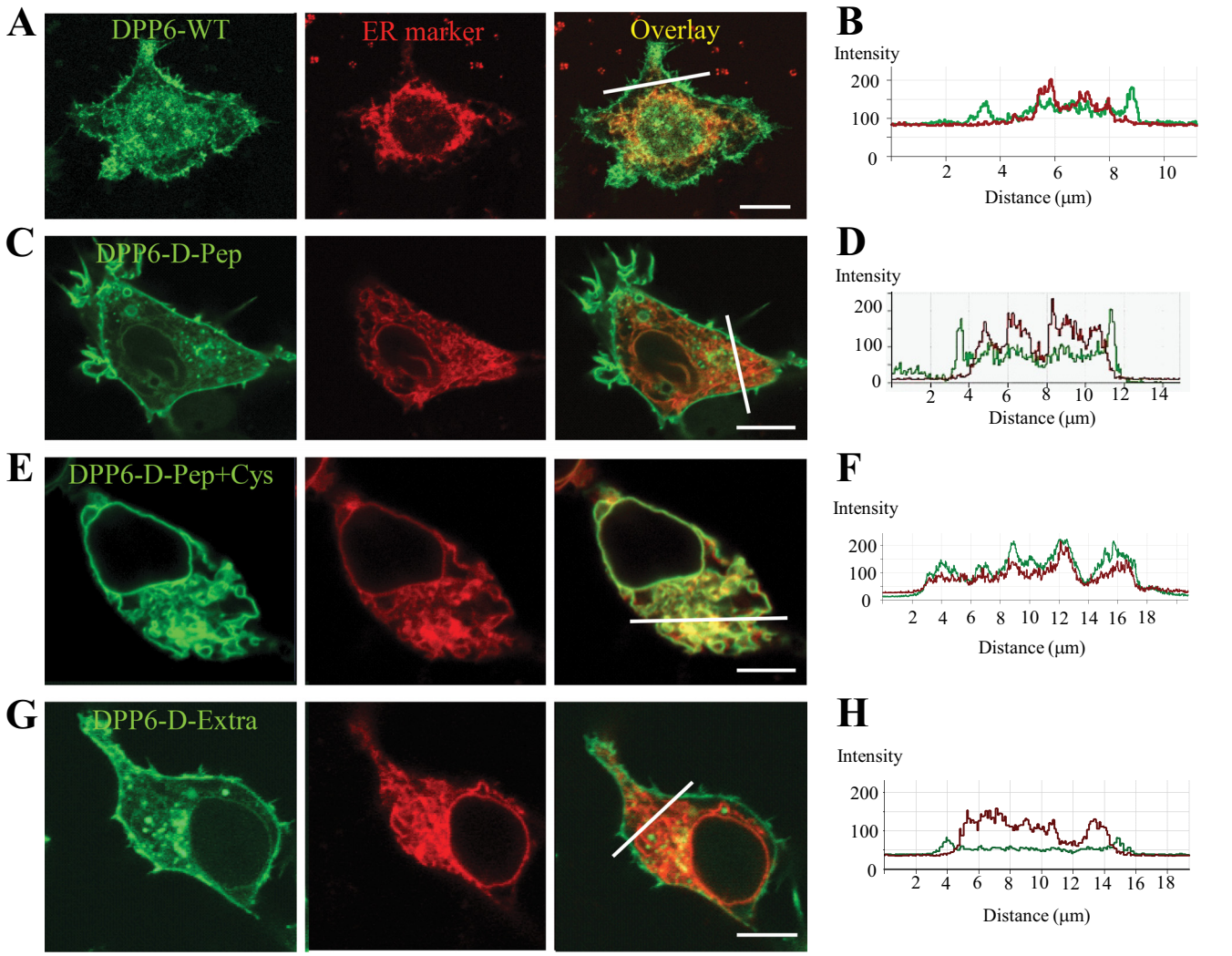

FIGURE 2. **The cysteine rich domain of DPP6 is important for DPP6 transporting from ER/Golgi to membrane.** Live cell imaging of HEK293 cells co-transfected with DPP6-WT or mutant construct (*green*) and an ER marker labeled with DsRed (*red*). Scale bars represent 10 μm. *A*, like in Fig. 1, DPP6-WT is expressed primarily along the membrane and shows little co-localization with the ER marker. *C*, DPP6-D-Pep is in the membrane similar as DPP6-WT in *A*. *E*, DPP6-D-Pep+Cys remain in ER and co-localized with ER marker. *G*, DPP6-D-Extra with ER marker show the distribution of the mutation is less in intracellular ER/Golgi compartment, but more surprised expressing in the membrane. An intensity plot along the *white line* is shown in *B*, *D*, *F*, and *H*.

that mutation DPP6-C349A/C356A colocalizes with the ER marker, but not with the membrane marker (Fig. 3, *D* and *E*). Similar results were found for DPP6-C465A+C468A (Fig. 4, *B* and *E*) and the double mutation of DPP6-C349A/C356A and C465A/C468A (images not shown). These findings were supported in a biotinylation assay showing that both single mutations and the double mutation DPP6-C349A/C356A + C465A/C468A have decreased surface expression compared with DPP6-WT (Fig. 3, *F* and *G*; Fig. 4, *F* and *G*). Together, these results indicate that both mutations individually play important roles in the transport of DPP6 from ER to the cell membrane but that these effects are not additive, implying that intact disulfide bridges are necessary for the proper folding of the protein.

C349/C356 and C465/C468 Disulfide Bridges of DPP6 Are Not Required for Interaction with Kv4.2, but Are Functionally Important—After finding that disulfide bridges in the cysteine rich domain are necessary for DPP6 transport from the ER to cell membrane we examined whether the disulfide bridges are important for DPP6 interaction with the primary subunit Kv4.2. We performed Co-IP experiment in COS7 cells, which were transfected with Kv4.2 and either DPP6-WT, DPP6-C349A/C356A, or DPP6-C349A/C356A+C465A/C468A. After pull-down with a Kv4.2 antibody, Western blot analysis showed that both single and double bridge mutants are still able to bind Kv4.2 (Fig. 5*A*). However, since the mutants get trapped in the ER they do not act to enhance Kv4.2 surface expression as DPP6-WT does, as evidenced in both biotinylation assays (Fig. 5, *B* and *C*) in COS7 cells and electrophysiological recordings from HEK293 cells (Fig. 5*D*). Peak current density of Kv4.2-mediated currents significantly increased after co-expression with DPP6 compared with the control (Fig. 5*D*; $p < 0.05$). In contrast, peak current density of Kv4.2 co-expressed with DPP6-C349A/C356A or DPP6-C349A/C356A+C465A/C468A showed no significant difference (Fig. 5*D*; $p > 0.05$). Together these data from the biochemical assay and the electrophysiological recording confirm that C349/C356 and C465/C468 disulfide bridges of DPP6 play a key role in the enhancement of Kv4.2 surface expression by DPP6 in these heterologous expression systems.

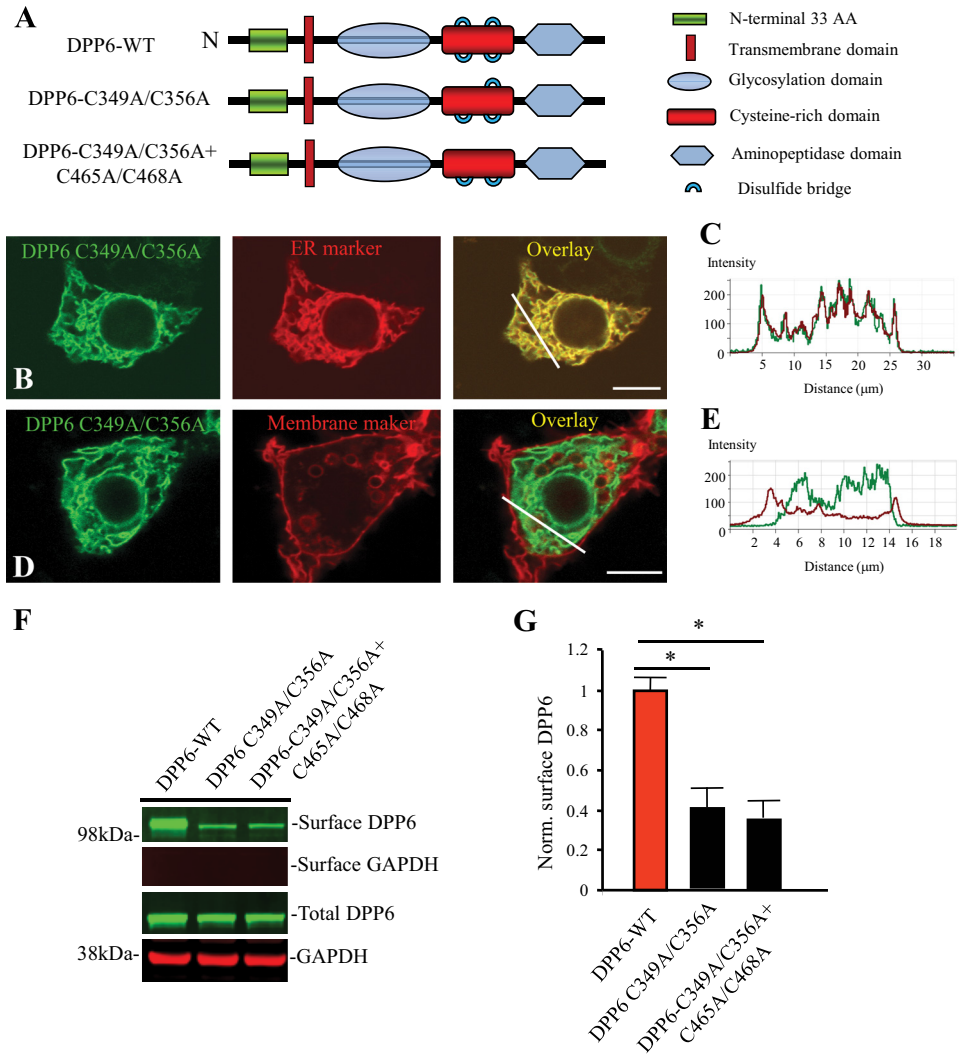

FIGURE 3. **Disulfide bridges of DPP6 are important for its localization on the plasma membrane.** *A*, domain structures of DPP6-WT and disulfide bridge mutations used in this study. *B*, live imaging of HEK cell shows the mutation DPP6-C349A/C356A co-localized with the ER marker. An intensity plot along the *white line* is shown in *C*. Scale bar represents 10 μm. *D*, DPP6-C349A/C356A shows no co-localization with the membrane marker. An intensity plot along the *white line* is shown in *E*. *F*, surface biotinylation assay in transfected COS7 cells. DPP6-C349A/C356A and DPP6-C349A/C356A+C465A/C468A had less surface expression than wild type. GAPDH served as a loading control and the surface negative control. *G*, pooled surface biotinylation data ($n = 6$), normalized to total protein level of DPP6. DPP6-C349A/C356A and DPP6-C349A/C356A+C465A/C468A have significantly reduced surface expression compared with wild type. Error bars represent S.E.

KChIPs Do Not Rescue Kv4.2 Membrane Expression with DPP6 Mutations—The two main classes of Kv4 auxiliary subunits are the DPP6 proteins and the K^+ channel-interacting proteins (KChIPs; (30)). A ternary complex of Kv4, DPP6, and Kv channel-interacting proteins (KChIPs) is thought to underlie the native A-type K^+ current in CA1 neurons (16). KChIPs also enhance Kv4.2 expression (31). Might KChIPs be able to rescue enhanced Kv4.2 expression with the mutant DPP6 proteins? To determine this, we compared the expression of Kv4.2 with Kv4.2+KChIP2a, Kv4.2+KChIP2a+DPP6 and Kv4.2+KChIP2a+DPP6 mutations DPP6-C349A/C356A or DPP6-C349A/C356A+C465A/C468A. Biotinylation results from COS7 cells showed the surface expression of Kv4.2 is increased about 3-fold by KChIP2a compared with control (Fig. 6, *A* and *B*, $p < 0.05$). Although DPP6-WT further increased membrane expression (Fig. 6, *A* and *B*; $p < 0.05$), the mutations of DPP6-C349A/C356A or DPP6-C349A/C356A+C465A/C468A abolished both the DPP6- and KChIP2-mediated enhancements (Fig. 6, *A* and *B*; $p < 0.05$). Similar results were found using KChIP3 (data not shown). These results were confirmed by measuring current density of Kv4.2 in HEK293 cells in electrophysiological recordings (Fig. 6*C*). That KChIP2 cannot rescue the trafficking effects of mutant DPP6 proteins seems to indicate that Kv4.2 complexing with DPP6 precedes that with KChIPs. This possibility is supported by our results showing that DPP6 mutants are trapped in the ER while a previous report found that KChIP proteins interact with Kv4.2 in post-ER vesicles (32). Taken together, these data show that there is a pool of Kv4.2 channels which reliably traffic to the surface without chaperone proteins but that both DPP6 and KChIP proteins, when properly folded, enhance the surface expression/stability of Kv4.2 channels.

The Short Intracellular N-terminal Plus Transmembrane Domains of DPP6 Are Necessary for Its Interaction and Modulation of Kv4.2—DPP6 interacts with Kv4 channels to dramatically increase Kv4 surface expression and accelerate

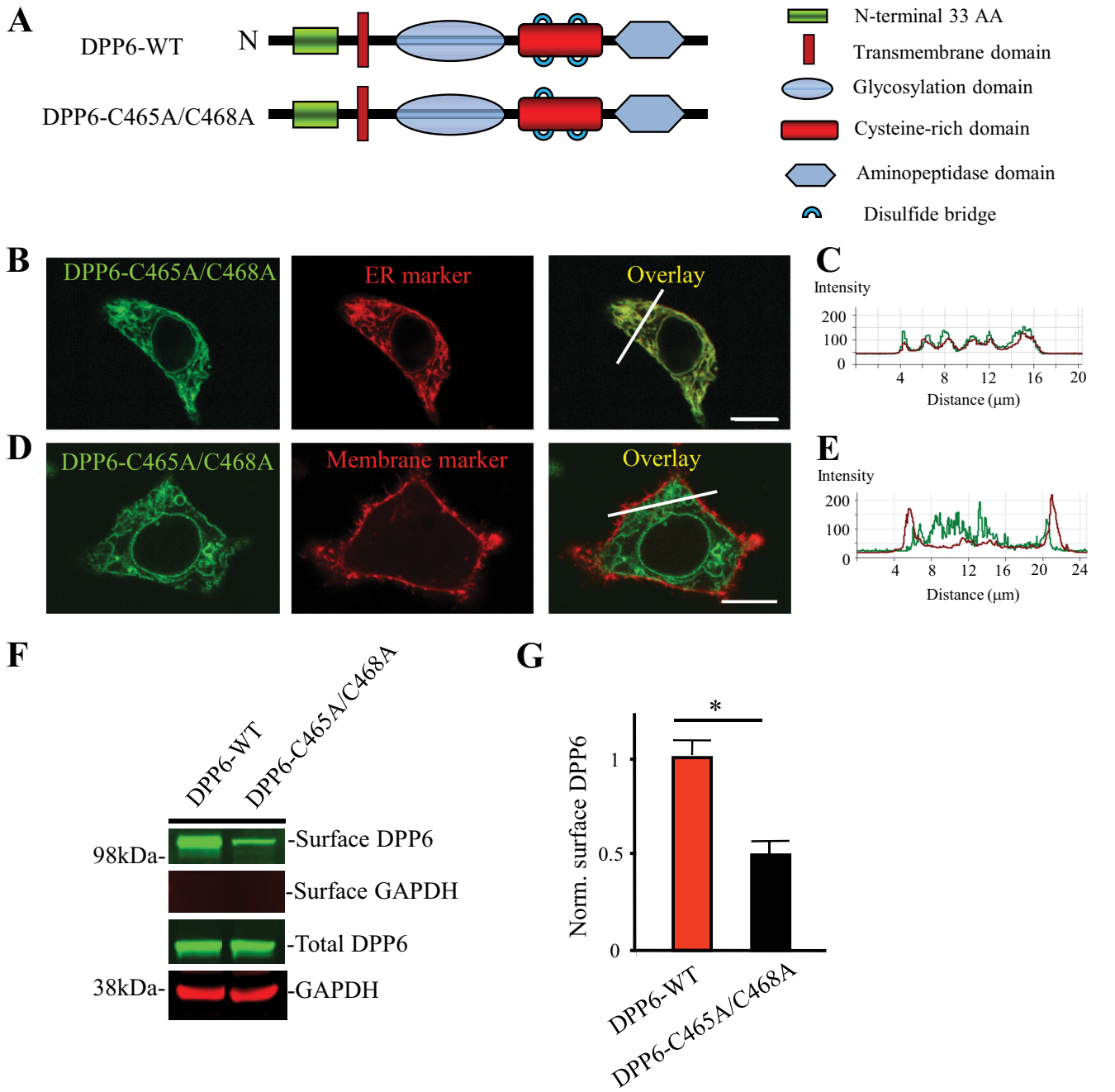

FIGURE 4. **A second disulfide bridge of DPP6 at C465/C468 is important for its localization on the plasma membrane.** *A*, domain structures of DPP6-WT and disulfide bridge mutations used in this study. Live cell imaging in HEK cells co-transfected with DPP6-C465A/C468A, a mutation of only the second disulfide bridge (*green*), and an ER or membrane marker (*red*). Scale bars represent 10 μm. DPP6-C465A/C468A shows colocalization with ER marker (*B*) and no colocalization with membrane marker (*D*). An intensity plot along the *white line* is shown in *C*, *E*. *F* and *G*, surface expression of DPP6-WT and mutation DPP6-C465A/C468A were measured with a biotinylation assay in overexpressed COS7 cells. Results showed that the surface expression of mutation DPP6-C465A/C468A is decreased compared with the DPP6-WT. GAPDH served as a loading control and the surface negative control ($p < 0.05$). *Error bars* represent S.E.

many properties of A-type channels including their activation, inactivation and recovery from inactivation. Here we examined which domain of DPP6 is important for its interaction with Kv4.2. We performed Co-IP experiments by co-transfecting Kv4.2 with a control vector, DPP6-WT, or DPP6-D-Extra in COS7 cells and pulling down with a Kv4.2 antibody. Western blot analysis showed that both DPP6-WT and the DPP6-D-Extra mutant bind to Kv4.2 (Fig. 7*B*). The entire extracellular C terminus of DPP6 therefore does not appear to be required for its binding with Kv4.2. To further localize the binding site, we generated two truncation mutants, an N-terminal deletion DPP6-D32 (32 aa at N terminus) or N-terminal plus transmembrane domain deletion DPP6-D54 (Fig. 7*A*). We performed Co-IP experiments in COS7 cells co-expressing Kv4.2 with either DPP6-WT, DPP6-D32 or DPP6-D54 (Fig. 7*C*). Western blot analysis showed that DPP6-D32 pulled down less Kv4.2, while DPP6-D54 prevented their interaction. These results suggest that the N-terminal and transmembrane domains of DPP6 are important for its interaction with Kv4.2.

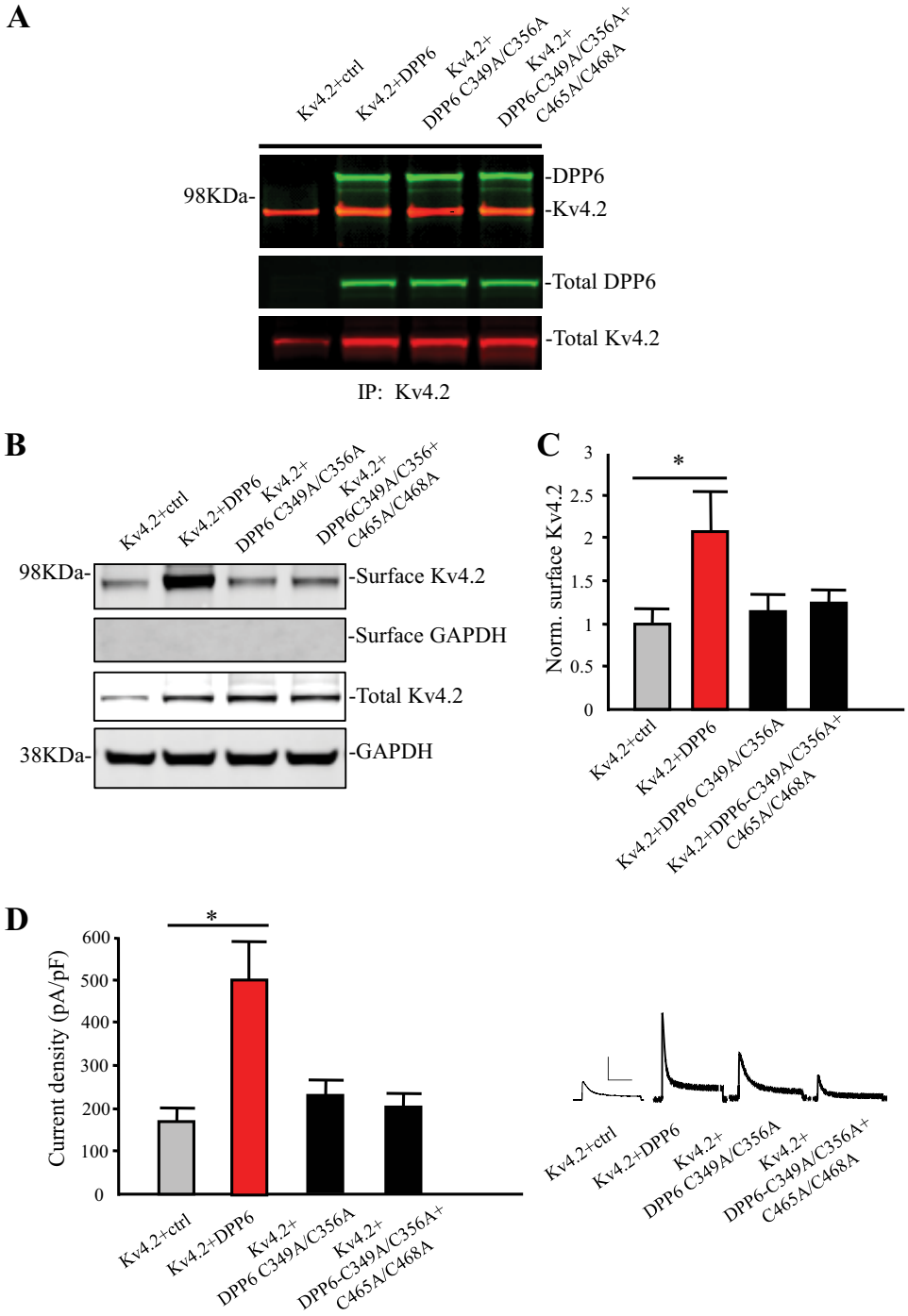

FIGURE 5. **DPP6 disulfide bridges in the cysteine rich-domain are important for increasing surface expression of Kv4. 2, but not for the interaction between DPP6 and Kv4.2.** *A*, disulfide bridges are not necessary for the interaction between DPP6 and Kv4.2. Co-immunoprecipitation assay in COS7 cells of Kv4.2 with control vector, DPP6-WT, DPP6-C349A/C356A, and DPP6-C349A/C356A+C465A/C468A. Cell lysate were pulled down using an anti-Kv4.2 antibody, and Western blots were probed with anti-Kv4.2 and anti-DPP6 antibodies and visualized by anti-mouse Alexa Fluor 680 secondary (*red*) and anti-rabbit Alexa Fluor 800 secondary (*green*) antibody. Total input of DPP6 and Kv4.2 expression showed, respectively. DPP6 was pulled down in all conditions, indicating that the disulfide mutants are still able to bind to Kv4.2. *B*, surface Kv4.2 were detected using a biotinylation assay in transfected COS7 cells. Cells co-expressing Kv4.2 with DPP6 showed much greater surface expression than for the expressing Kv4.2 alone with control. Surface expression of the Kv4.2 was not enhanced by either DPP6-C349A/C356A or DPP6-C349A/C356A+C465A/C468A co-expression. GAPDH served as a loading control and the surface negative control. *C*, pooled surface biotinylation data ($n = 6$), normalized to total protein level of Kv4.2. DPP6-WT increases surface Kv4.2 expression about 2-fold over control conditions, but there is no significant difference between control and disulfide mutants. Error bars represent S.E. *D*, effects of DPP6 and mutation DPP6-C349A/C356A and DPP6 C349A/C356A+C465A/C468A on I_A. HEK293 cells were co-transfected with Kv4.2 and DPP6 or a disulfide mutation. Peak amplitude of I_A was recorded and divided by cell capacitance to calculate current density (pA/pF). Cells co-transfected with Kv4.2 and DPP6 ($n = 12$) showed a significant increase in current density($p < 0.01$)when compared with control ($n = 13$). Cells co-transfected with Kv4.2 and DPP6-C349A/C356A ($n = 12$) also showed a significant increase in current density ($p = 0.014$), however the increase was not as obvious as with DPP6. Cells co-transfected with Kv4.2 and DPP6-C349A/C356A+C465A/C468A ($n = 13$) did not show an increase in current density ($p = 0.5$).

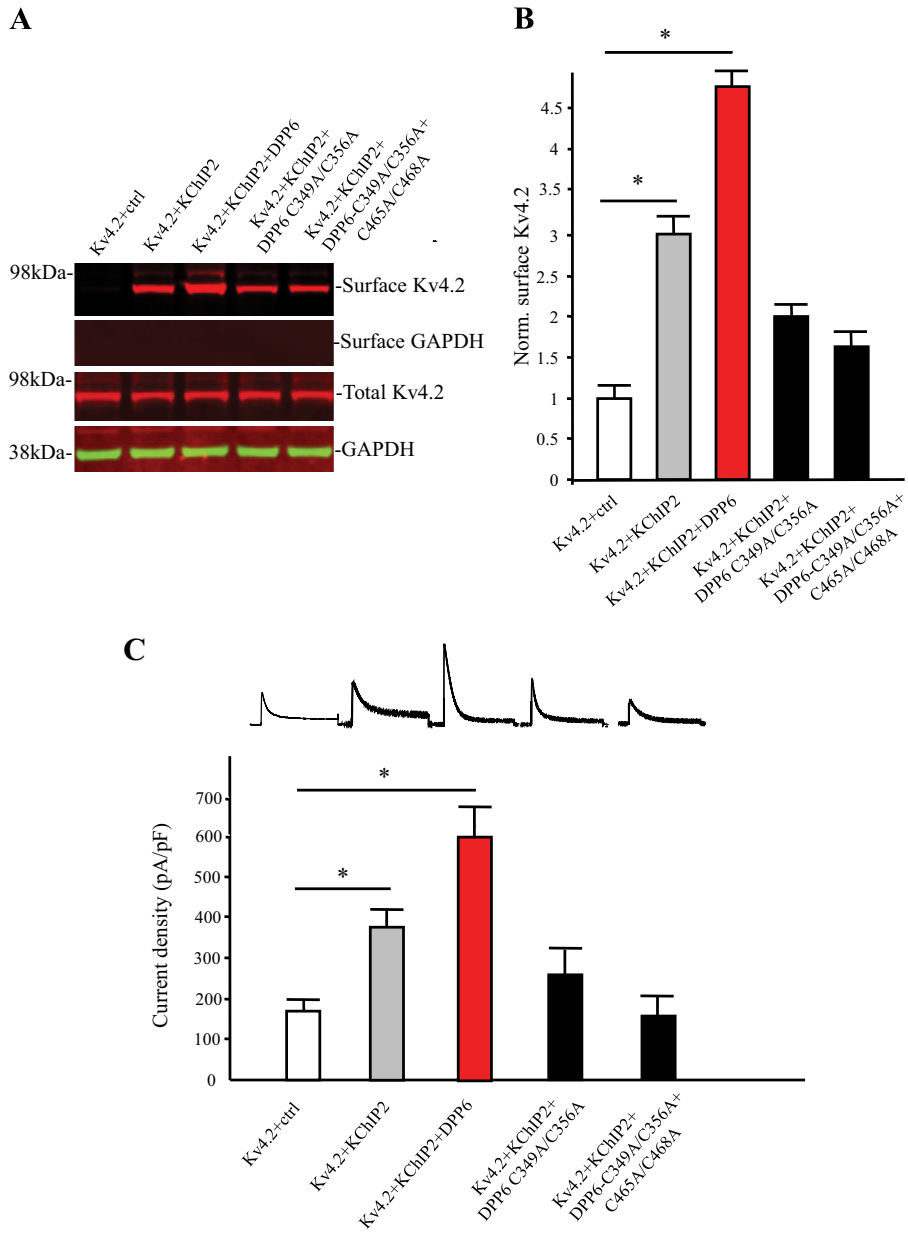

FIGURE 6. **DPP6 increase in Kv4.2 surface expression with KChIP2 requires the disulfide bridge in the cysteine rich-domain.** *A*, surface biotinylation assay in transfected COS7 cells. Cells co-expressing Kv4.2, KChIP2a, and DPP6 showed much greater Kv4.2 surface expression than those expressing Kv4.2 alone or with only KChIP2a. Surface expression of Kv4.2 was not enhanced by either DPP6-C349A/C356A or DPP6-C349A/C356A+C465A/C468A co-expression. GAPDH served as a loading control and the surface negative control. *B*, pooled data ($n = 4$) normalized to total Kv4.2 expression shows that DPP6 co-expression increases surface Kv4.2 expression in the presence of KChIP2a about 4-fold. Error bars represent S.E. *C*, I_A current density was measured in HEK293 cells expressing Kv4.2, KChIP2a, and either DPP6-WT or disulfide mutations. Cells were co-transfected with Kv4.2 and either empty vector ($n = 10$), KChIP2a ($n = 10$), DPP6 + KChIP2a ($n = 10$), DPP6-C349A/C356A+ KChIP2a ($n = 10$), or DPP6-C465A/C468A + KChIP2a ($n = 11$). KChIP2a alone and in combination with DPP6 achieved a significant increase in Kv4.2 current density ($p < 0.01$) when compared with the control. KChIP2a + DPP6-C349A/C356A or DPP6 DPP6-C349A/C356A+C465A/C468A did not cause a significant change in Kv4.2 current density when compared with control ($p = 0.24$, $p = 0.91$, respectively).

Previously we found that deleting the entire extracellular domain of DPP6 (DPP6-D-Extra) showed some membrane expression (Figs. 1 and 2). As we found that the extracellular domain of DPP6 is not important for its interaction with Kv4.2, we investigated whether the extracellular domain of DPP6 is required for its regulation of Kv4.2's electrophysiological properties. Electrophysiological recordings of Kv4.2's recovery from inactivation were performed in HEK293 cells (Fig. 7, *D* and *E*). Recovery from inactivation was, as expected, significantly faster for cells co-expressing Kv4.2 and DPP6-WT ($n = 9$) compared with the Kv4.2 with a GFP control ($n = 7$, $p < 0.05$). Interestingly, recovery from inactivation was also significantly faster when Kv4.2 was co-expressed with DPP6-D-Extra ($n = 6$, $p < 0.05$) and nearly identical to that found in DPP6-WT recordings. These findings indicate that the N-terminal intracellular domain of DPP6, but not the entire extracellular domain, is necessary for interaction and acceleration of Kv4.2 channel properties.

Finally, we examined which extracellular domains of DPP6 affect its function to enhance the surface expression of Kv4.2. We performed biotinylation assays in COS7 cells transfected with Kv4.2 and either a control plasmid, DPP6-WT or the other

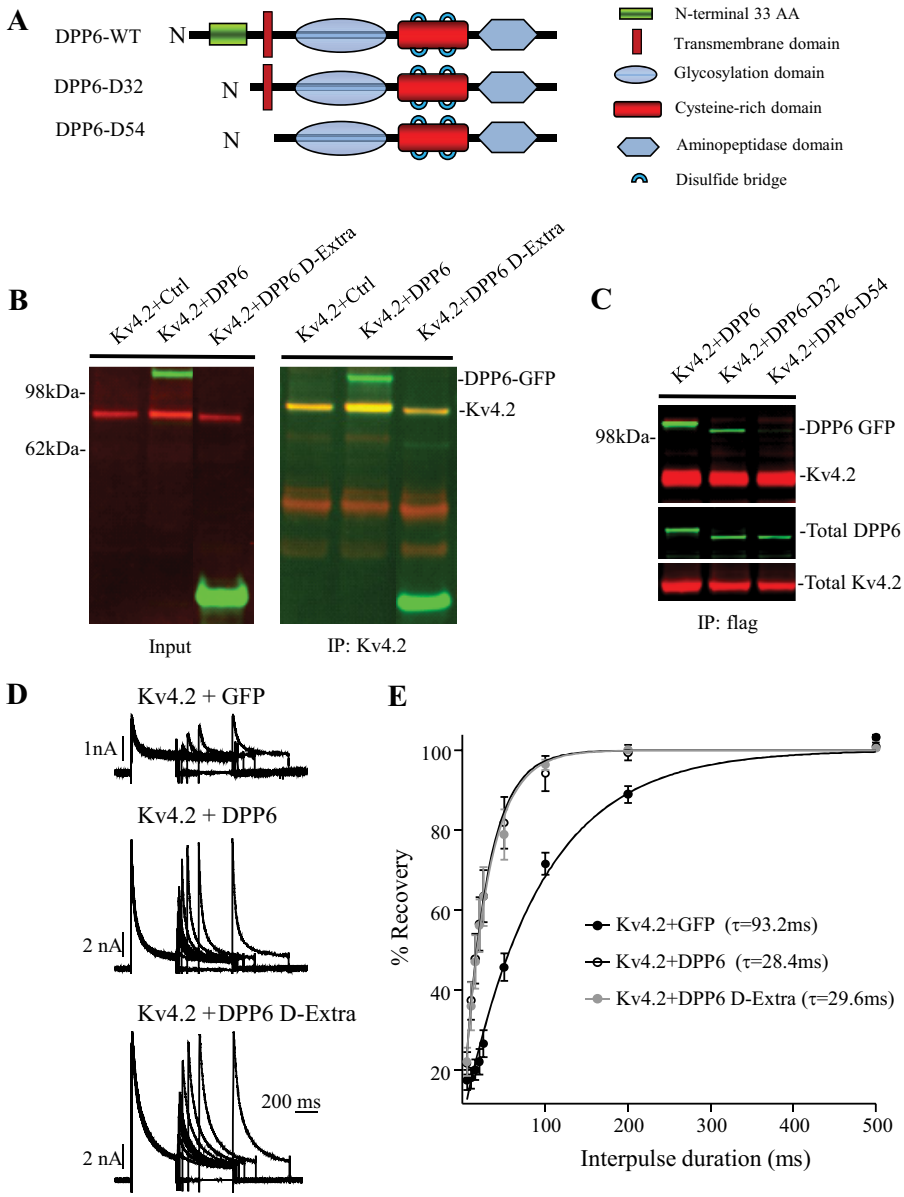

FIGURE 7. **The DPP6 N terminus and transmembrane domain are necessary for its interaction with Kv4. 2.** *A*, domain structures of wild type DPP6 and the N-terminal truncation deletions used in this study. *B*, co-IP assay in COS7 cells co-transfected with Kv4.2 and control, DPP6-WT or DPP6-D-Extra. Cell lysates were pulled down with anti-Kv4.2. DPP6-D-Extra was pulled down, indicating that the C-terminal extracellular domain of DPP6 is not necessary for its interaction with Kv4.2. *C*, Co-IP assay in COS7 cells co-transfected with Kv4.2-Flag and DPP6-WT or N-terminal deletions D32 and D54. Cell lysates were pulled down by anti-Flag. Results show that the N terminus plus transmembrane domains of DPP6 are required for its interaction with Kv4.2. Inputs show the total expression of Kv4.2 and DPP6 in COS7 cells. Western blots were probed with anti-Kv4.2 antibody (1:2000) or anti-DPP6 antibody (1:2000) and visualized by anti-mouse Alexa Fluor 680 and anti-rabbit Alexa Fluor 800 secondary antibody, respectively. Inputs show the total expression of Kv4.2 and DPP6 in COS7 cells. *D* and *E*, I_A recovery from inactivation was measured in HEK 293 cells co-transfected with Kv4.2 and control vector, DPP6-WT, or DPP6-D-Extra. Electrophysiological experiments were used to determine the impact of these conditions on the recovery from inactivation of the Kv4.2 current. Representative traces are displayed in *D*. In *E*, recovery percentage was calculated by dividing the second peak by the initial peak and plotted by delay between sweeps. Time to full I_A recovery was much faster in cells co-transfected with Kv4.2 and DPP6-WT ($n = 9$) than the control ($n = 7$). Kv4.2 and DPP6-D-Extra ($n = 6$) also showed a significant acceleration in recovery from inactivation and was not significantly different from Kv4.2 and DPP6-WT. *Error bars* represent S.E.

C-terminal deletions (Fig. 8*A*). The surface expression of Kv4.2 was enhanced by DPP6-WT and DPP6-D-Pep, but not by DPP6-D-Pep+Cys and DPP6-D-Extra. When normalized to the total Kv4.2 expression, surface Kv4.2 was significantly increased compared with the Kv4.2 with control (vector) when co-expressed with DPP6-WT and DPP6-D-Pep (Fig. 8*B*, $p < 0.05$), but not with DPP6-D-Pep+Cys and DPP6-D-Extra (Fig. 8*B*, $p > 0.05$). These results suggest that, as for DPP6 itself (Figs. 1 and 2), the cysteine-rich domain of DPP6 plays an important role in allowing forward trafficking of Kv4.2 out of the ER, even though it is not necessary for their interaction.

The previous results showed that the cysteine rich domain of DPP6 is important to increase the surface expression of Kv4.2. Next we tested whether the enhanced surface expression of Kv4.2 is caused by enhanced total Kv4.2 stabilization. We measured the stability of Kv4.2 subunits in stabilization experiments with COS7 cells which were co-transfected with Kv4.2 and control, DPP6-WT, DPP6-D-Pep, DPP6-D-Pep+Cys, or

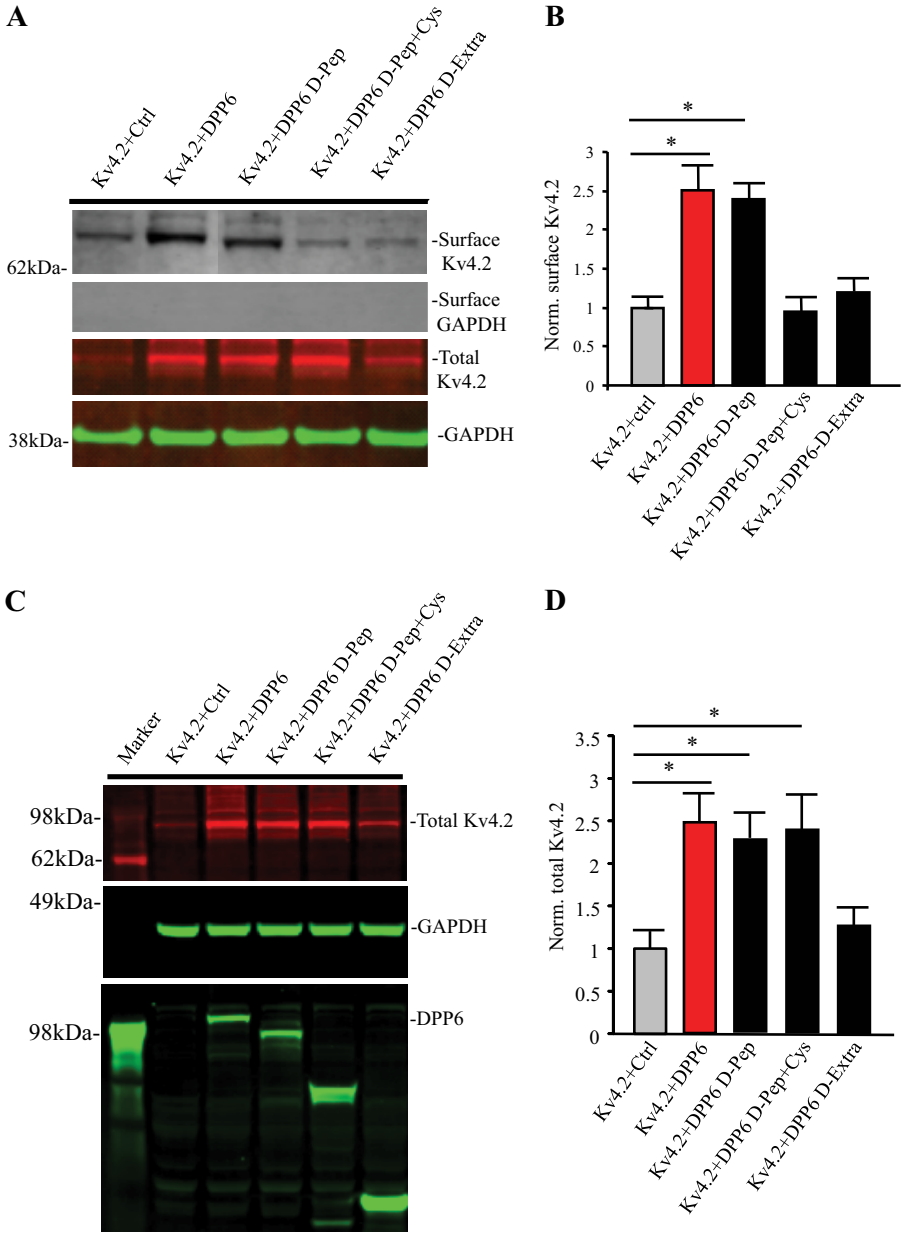

FIGURE 8. **DPP6-mediated increase in Kv4. 2 surface expression requires the cysteine-rich domain.** *A*, surface Kv4.2 biotinylation assay in COS7 cells. Kv4.2 and DPP6-WT or DPP6-D-Pep show greater surface expression than for Kv4.2 and control. Surface expression of the Kv4.2 was not enhanced by co-expression of either DPP6-D-Pep+Cys or DPP6-D-Extra. GAPDH served as a loading control and the surface negative control. *B*, pooled data ($n = 4$) normalized to total Kv4.2 expression shows that DPP6-WT and DPP6-D-Pep increase surface Kv4.2 expression by about 2-fold. Error bars represent S.E. *C*, entire extracellular domain of DPP6 is necessary to enhance Kv4.2 stability. The total expression level of Kv4.2 was measured in stabilization experiments performed in COS7 cells. The normalized total protein level of Kv4.2 was significantly increased by co-expression of Kv4.2 with DPP6-WT, DPP6-D-Pep, DPP6-D-Pep+Cys as compared with control. In contrast, the normalized Kv4.2 levels were not changed when co-expressed with DPP6-D-Extra. *D*, pooled data ($n = 6$) normalized to total Kv4.2 expression shows that DPP6-WT, DPP6-D-Pep, and DPP6-D-Pep+Cys enhanced stability of Kv4.2 expression by about 2-fold, but DPP6-D-Extra did not. Error bars represent S.E.

DPP6-D-Extra (Fig. 8*C*). Normalized Kv4.2 protein levels were increased ~2-fold after co-transfection with DPP6-WT, as well with mutations DPP6-D-Pep and DPP6-D-Pep+Cys compared with the total level of Kv4.2 with control (Fig. 8*D*, $p < 0.05$). In contrast, normalized Kv4.2 levels were significantly decreased when co-transfected with DPP6-D-Extra mutation compared with DPP6-WT. Together these results show that the cysteine-rich domain is necessary for the forward trafficking of Kv4.2/DPP6 complexes out of the ER. It is likely that this is because the cysteine-rich domain is required for the proper folding of the protein. In addition, we found that the glycosylation domain, but not the cysteine-rich domain, is necessary to enhance total protein levels, compared with Kv4.2 by itself.

DISCUSSION

DPP6 Domains Responsible for Its Transport—In this study we examined the functional role of distinct domains within the structure of the transmembrane protein DPP6. We found that the extracellular, cysteine-rich domain of DPP6 is required for its trafficking out of the ER (Figs. 1 and 2). Either of two disul-

fide bridges (C349/C356 and C465/C468) in this region resulted in ER retention (Figs. 3 and 4), implying that proper folding of the protein is required for exit. Interestingly, a more severe deletion of the entire extracellular domain allowed membrane expression, perhaps indicating an ER-retention domain in the interceding glycosylation domain. ER retention was not rescued by co-expression with another prominent Kv4.2 accessory subunit KChIP2 (Fig. 6).

DPP6 Domains Responsible for Its Interaction and Function in Kv4 Complexes—As shown previously (20, 21), we found that DPP6-WT associates with Kv4.2 increasing its surface expression and accelerating its recovery from inactivation in HEK293 cells (Figs. 5, 7, and 8). Here we extend these results to show which domains are required for each function of DPP6. DPP6 association with Kv4.2 requires DPP6 N-terminal plus transmembrane domains (54 aa, Fig. 7). Interestingly, this domain fully replicated DPP6 functional effect of accelerating Kv4.2 recovery from inactivation in HEK293 cells (Fig. 7). Our results support a previous report (33) which used chimeric proteins to identify a region of the DPP family member DPPY (DPP10) from its N terminus to the end of its transmembrane domain to interact with another Kv4 family member, Kv4.3.

Although we found Kv4.2 to interact with the N-terminal and transmembrane domains of DPP6, we did not find their co-expression to result in enhanced Kv4.2 surface expression. To increase surface Kv4.2 beyond basal levels required the intact extracellular, cysteine-rich domain but not the extracellular aminopeptidase domain (Fig. 8, *A* and *B*). Data from biochemical and electrophysiological recordings confirmed that intact disulfide bridges of DPP6 (C349/C356 and C465/C46) are necessary to enhance Kv4.2 surface expression by DPP6 in these heterologous expression systems (Fig. 5). In contrast, total Kv4.2 protein was not affected by loss the cysteine-rich domain but did require the glycoslyation domain (Fig. 8, *C* and *D*) perhaps indicating that the unglycosylated protein degrades quickly.

Together, these results suggest that there exist multiple pools of Kv4.2 channels. First, a basal pool of Kv4.2 is able to traffic out of the ER without binding any accessory subunits. Although caution is warranted in extrapolating results obtained in heterologous expression systems to the native environment, this finding was suggested previously in a study investigating the effect of knocking out DPP6 on A-channel expression in hippocampal CA1 pyramidal neuron dendrites (22). Our results presented here suggest a second pool of Kv4.2 channels, which bind with DPP6 in the ER, resulting in increased surface expression of Kv4.2. This pool may correspond to the enhanced A-current found in distal CA1 dendrites of wild type but not DPP6 knock out mice (22).

Once out of the ER, Kv4-DPP6 channels can be further modulated by interaction with KChIP auxiliary subunits in a post ER vesicular pathway (32). Knockdown of DPP6 in cerebellar granule neurons and hippocampal pyramidal neurons results in a loss of both Kv4.2 and KChIP3 (24) suggesting that DPP6 may be required for Kv4 interaction with KChIPs.

Potential DPP6 Domains Responsible for Its Role in Neurodevelopment—We have recently published evidence indicating a role for DPP6 in neurodevelopment, which appears to be independent of its role as a Kv4 auxiliary subunit (11). In that study we found dendritic filopodia formation and stability to be impacted in DPP6-KO mice. Other groups have also found indications that DPP6, like its related, structurally similar family member DPPIV, is a multifunctional protein. Foeger *et al.* (2012) found that heterologously expressed DPP6 localizes to the cell surface in the absence of Kv4.2 in mouse cortex (23) while Nadin and Pfaffinger (34) reported that DPP6 interacts with the K2P channel TASK-3 to regulate resting membrane potential and input resistance in cerebellar granule cells (34). Moreover numerous genome-wide association screens for a variety of maladies implicate a potential role for DPP6 (26, 27, 35, 36). Further studies will be required to determine which DPP6 domains are responsible for its various functions but it seems likely that its role in regulating filopodia involves an interaction between its β-propeller structure located in the cysteine-rich domain and the extracellular matrix protein fibronectin (11) as found for DPPIV (10) (37). Future studies may also address the role of the non-functional aminopeptidase domain of DPP6, which did not greatly impact protein trafficking in the present study.

Acknowledgment—We thank Vincent Schram in the NICHD Microscopy & Imaging Core for technical assistance.

REFERENCES

1. Strop, P., Bankovich, A. J., Hansen, K. C., Garcia, K. C., and Brunger, A. T. (2004) Structure of a human A-type potassium channel interacting protein DPPX, a member of the dipeptidyl aminopeptidase family. *J. Mol. Biol.* **343,** 1055–1065
2. Kin, Y., Misumi, Y., and Ikehara, Y. (2001) Biosynthesis and characterization of the brain-specific membrane protein DPPX, a dipeptidyl peptidase IV-related protein. *J. Biochem.* **129,** 289–295
3. De Meester, I., Korom, S., Van Damme, J., and Scharpé, S. (1999) CD26, let it cut or cut it down. *Immunol. Today* **20,** 367–375
4. Hildebrandt, M., Rose, M., Mayr, C., Arck, P., Schüler, C., Reutter, W., Salama, A., and Klapp, B. F. (2000) Dipeptidyl peptidase IV (DPP IV, CD26) in patients with mental eating disorders. *Adv. Exp. Med. Biol.* **477,** 197–204
5. Gorrell, M. D., Gysbers, V., and McCaughan, G. W. (2001) CD26: a multifunctional integral membrane and secreted protein of activated lymphocytes. *Scand. J. Immunol.* **54,** 249–264
6. Yokotani, N., Doi, K., Wenthold, R. J., and Wada, K. (1993) Non-conservation of a catalytic residue in a dipeptidyl aminopeptidase IV-related protein encoded by a gene on human chromosome 7. *Hum. Mol. Genet.* **2,** 1037–1039
7. Nadal, M. S., Amarillo, Y., Vega-Saenz de Miera, E., and Rudy, B. (2006) Differential characterization of three alternative spliced isoforms of DPPX. *Brain Res.* **1094,** 1–12
8. Nadal, M. S., Ozaita, A., Amarillo, Y., Vega-Saenz de Miera, E., Ma, Y., Mo, W., Goldberg, E. M., Misumi, Y., Ikehara, Y., Neubert, T. A., and Rudy, B. (2003) The CD26-related dipeptidyl aminopeptidase-like protein DPPX is a critical component of neuronal A-type K+ channels. *Neuron* **37,** 449–461
9. Löster, K., Zeilinger, K., Schuppan, D., and Reutter, W. (1995) The cysteine-rich region of dipeptidyl peptidase IV (CD 26) is the collagen-binding site. *Biochem. Biophys. Res. Commun.* **217,** 341–348
10. Cheng, H. C., Abdel-Ghany, M., and Pauli, B. U. (2003) A novel consensus motif in fibronectin mediates dipeptidyl peptidase IV adhesion and metastasis. *J. Biol. Chem.* **278,** 24600–24607
11. Lin, L., Sun, W., Throesch, B., Kung, F., Decoster, J. T., Berner, C. J., Cheney, R. E., Rudy, B., and Hoffman, D. A. (2013) DPP6 regulation of dendritic morphogenesis impacts hippocampal synaptic development.

Nat. Commun. **4,** 2270
12. Shah, M. M., Hammond, R. S., and Hoffman, D. A. (2010) Dendritic ion channel trafficking and plasticity. *Trends Neurosci.* **33,** 307–316
13. Chen, X., Yuan, L. L., Zhao, C., Birnbaum, S. G., Frick, A., Jung, W. E., Schwarz, T. L., Sweatt, J. D., and Johnston, D. (2006) Deletion of Kv4.2 gene eliminates dendritic A-type K+ current and enhances induction of long-term potentiation in hippocampal CA1 pyramidal neurons. *J. Neurosci.* **26,** 12143–12151
14. Kim, J., Wei, D. S., and Hoffman, D. A. (2005) Kv4 potassium channel subunits control action potential repolarization and frequency-dependent broadening in rat hippocampal CA1 pyramidal neurones. *J. Physiol.* **569,** 41–57
15. Kim, J., Jung, S. C., Clemens, A. M., Petralia, R. S., and Hoffman, D. A. (2007) Regulation of dendritic excitability by activity-dependent trafficking of the A-type K+ channel subunit Kv4.2 in hippocampal neurons. *Neuron* **54,** 933–947
16. Maffie, J., and Rudy, B. (2008) Weighing the evidence for a ternary protein complex mediating A-type K+ currents in neurons. *J. Physiol.* **586,** 5609–5623
17. Jerng, H. H., Kunjilwar, K., and Pfaffinger, P. J. (2005) Multiprotein assembly of Kv4.2, KChIP3 and DPP10 produces ternary channel complexes with ISA-like properties. *J. Physiol.* **568,** 767–788
18. Rhodes, K. J., Carroll, K. I., Sung, M. A., Doliveira, L. C., Monaghan, M. M., Burke, S. L., Strassle, B. W., Buchwalder, L., Menegola, M., Cao, J., An, W. F., and Trimmer, J. S. (2004) KChIPs and Kv4 α subunits as integral components of A-type potassium channels in mammalian brain. *J. Neurosci.* **24,** 7903–7915
19. Zagha, E., Ozaita, A., Chang, S. Y., Nadal, M. S., Lin, U., Saganich, M. J., McCormack, T., Akinsanya, K. O., Qi, S. Y., and Rudy, B. (2005) DPP10 modulates Kv4-mediated A-type potassium channels. *J. Biol. Chem.* **280,** 18853–18861
20. Kim, J., Nadal, M. S., Clemens, A. M., Baron, M., Jung, S. C., Misumi, Y., Rudy, B., and Hoffman, D. A. (2008) Kv4 accessory protein DPPX (DPP6) is a critical regulator of membrane excitability in hippocampal CA1 pyramidal neurons. *J. Neurophysiol.* **100,** 1835–1847
21. Jerng, H. H., Pfaffinger, P. J., and Covarrubias, M. (2004) Molecular physiology and modulation of somatodendritic A-type potassium channels. *Mol. Cell Neurosci.* **27,** 343–369
22. Sun, W., Maffie, J. K., Lin, L., Petralia, R. S., Rudy, B., and Hoffman, D. A. (2011) DPP6 Establishes the A-Type K(+) Current Gradient Critical for the Regulation of Dendritic Excitability in CA1 Hippocampal Neurons. *Neuron* **71,** 1102–1115
23. Foeger, N. C., Norris, A. J., Wren, L. M., and Nerbonne, J. M. (2012) Augmentation of Kv4.2-encoded currents by accessory dipeptidyl peptidase 6 and 10 subunits reflects selective cell surface Kv4.2 protein stabilization. *J. Biol. Chem.* **287,** 9640–9650
24. Nadin, B. M., and Pfaffinger, P. J. (2010) Dipeptidyl peptidase-like protein 6 is required for normal electrophysiological properties of cerebellar granule cells. *J. Neurosci.* **30,** 8551–8565
25. Marshall, C. R., Noor, A., Vincent, J. B., Lionel, A. C., Feuk, L., Skaug, J., Shago, M., Moessner, R., Pinto, D., Ren, Y., Thiruvahindrapduram, B., Fiebig, A., Schreiber, S., Friedman, J., Ketelaars, C. E., Vos, Y. J., Ficicioglu, C., Kirkpatrick, S., Nicolson, R., Sloman, L., Summers, A., Gibbons, C. A., Teebi, A., Chitayat, D., Weksberg, R., Thompson, A., Vardy, C., Crosbie, V., Luscombe, S., Baatjes, R., Zwaigenbaum, L., Roberts, W., Fernandez, B., Szatmari, P., and Scherer, S. W. (2008) Structural variation of chromosomes in autism spectrum disorder. *Am. J. Hum. Genet.* **82,** 477–488
26. Noor, A., Whibley, A., Marshall, C. R., Gianakopoulos, P. J., Piton, A., Carson, A. R., Orlic-Milacic, M., Lionel, A. C., Sato, D., Pinto, D., Drmic, I., Noakes, C., Senman, L., Zhang, X., Mo, R., Gauthier, J., Crosbie, J., Pagnamenta, A. T., Munson, J., Estes, A. M., Fiebig, A., Franke, A., Schreiber, S., Stewart, A. F., Roberts, R., McPherson, R., Guter, S. J., Cook, E. H., Jr., Dawson, G., Schellenberg, G. D., Battaglia, A., Maestrini, E., Jeng, L., Hutchison, T., Rajcan-Separovic, E., Chudley, A. E., Lewis, S. M., Liu, X., Holden, J. J., Fernandez, B., Zwaigenbaum, L., Bryson, S. E., Roberts, W., Szatmari, P., Gallagher, L., Stratton, M. R., Gecz, J., Brady, A. F., Schwartz, C. E., Schachar, R. J., Monaco, A. P., Rouleau, G. A., Hui, C. C., Lucy Raymond, F., Scherer, S. W., and Vincent, J. B. (2010) Disruption at the PTCHD1 Locus on Xp22.11 in Autism spectrum disorder and intellectual disability. *Sci. Transl. Med.* **2,** 49ra68
27. Liao, C., Fu, F., Li, R., Yang, W. Q., Liao, H. Y., Yan, J. R., Li, J., Li, S. Y., Yang, X., and Li, D. Z. (2013) Loss-of-function variation in the DPP6 gene is associated with autosomal dominant microcephaly and mental retardation. *Eur. J. Med. Genet.* **56,** 484–489
28. van Es, M. A., van Vught, P. W., Blauw, H. M., Franke, L., Saris, C. G., Van den Bosch, L., de Jong, S. W., de Jong, V., Baas, F., van't Slot, R., Lemmens, R., Schelhaas, H. J., Birve, A., Sleegers, K., Van Broeckhoven, C., Schymick, J. C., Traynor, B. J., Wokke, J. H., Wijmenga, C., Robberecht, W., Andersen, P. M., Veldink, J. H., Ophoff, R. A., and van den Berg, L. H. (2008) Genetic variation in DPP6 is associated with susceptibility to amyotrophic lateral sclerosis. *Nat. Genet.* **40,** 29–31
29. Cronin, S., Berger, S., Ding, J., Schymick, J. C., Washecka, N., Hernandez, D. G., Greenway, M. J., Bradley, D. G., Traynor, B. J., and Hardiman, O. (2008) A genome-wide association study of sporadic ALS in a homogenous Irish population. *Hum. Mol. Genet.* **17,** 768–774
30. Jerng, H. H., Qian, Y., and Pfaffinger, P. J. (2004) Modulation of Kv4.2 channel expression and gating by dipeptidyl peptidase 10 (DPP10). *Biophys. J.* **87,** 2380–2396
31. An, W. F., Bowlby, M. R., Betty, M., Cao, J., Ling, H. P., Mendoza, G., Hinson, J. W., Mattsson, K. I., Strassle, B. W., Trimmer, J. S., and Rhodes, K. J. (2000) Modulation of A-type potassium channels by a family of calcium sensors. *Nature* **403,** 553–556
32. Hasdemir, B., Fitzgerald, D. J., Prior, I. A., Tepikin, A. V., and Burgoyne, R. D. (2005) Traffic of Kv4 K+ channels mediated by KChIP1 is via a novel post-ER vesicular pathway. *J. Cell Biol.* **171,** 459–469
33. Ren, X., Hayashi, Y., Yoshimura, N., and Takimoto, K. (2005) Transmembrane interaction mediates complex formation between peptidase homologues and Kv4 channels. *Mol Cell Neurosci.* **29,** 320–332
34. Nadin, B. M., and Pfaffinger, P. J. (2013) A new TASK for Dipeptidyl Peptidase-like Protein 6. *PloS one* **8,** e60831
35. Buzanskas, M. E., Grossi, D. A., Ventura, R. V., Schenkel, F. S., Sargolzaei, M., Meirelles, S. L., Mokry, F. B., Higa, R. H., Mudadu, M. A., da Silva, M. V., Niciura, S. C., Júnior, R. A., Alencar, M. M., Regitano, L. C., and Munari, D. P. (2014) Genome-wide association for growth traits in Canchim beef cattle. *PloS one* **9,** e94802
36. Sun, Y., Liu, R., Zhao, G., Zheng, M., Yu, X., Li, P., and Wen, J. (2014) Genome-wide linkage analysis and association study identifies Loci for polydactyly in chickens. *G3* **4,** 1167–1172
37. Cheng, H. C., Abdel-Ghany, M., Elble, R. C., and Pauli, B. U. (1998) Lung endothelial dipeptidyl peptidase IV promotes adhesion and metastasis of rat breast cancer cells via tumor cell surface-associated fibronectin. *J. Biol. Chem.* **273,** 24207–24215